applied sciences

MDPI

Article

Temperature Impact on Engineered Cementitious Composite Containing Basalt Fibers

Pouya Rafiei [1], Hoofar Shokravi [2], Seyed Esmaeil Mohammadyan-Yasouj [1,*], Seyed Saeid Rahimian Koloor [3] and Michal Petrů [4]

[1] Department of Civil Engineering, Najafabad Branch, Islamic Azad University, Najafabad 8514143131, Iran; pouya.rafiei72@gmail.com
[2] Faculty of Engineering, School of Civil Engineering, Universiti Teknologi Malaysia, Skudai 81310, Johor, Malaysia; shokravihoofar@utm.my
[3] Institute for Nanomaterials, Advanced Technologies and Innovations, Technical University of Liberec, Studentska 2, 46117 Liberec, Czech Republic; s.s.r.koloor@gmail.com
[4] Center for Nanomaterials, Advanced Technologies and Innovations, Technical University of Liberec, Studentska 2, 46117 Liberec, Czech Republic; michal.petru@tul.cz
* Correspondence: semy2016@pci.iaun.ac.ir

Abstract: Engineered cementitious composite (ECC) is a new generation of fiber-reinforced concrete with high ductility and exceptional crack control capabilities. However, ECC can suffer a substantial reduction in ductility when exposed to elevated temperatures resulting in a loss of crack-bridging ability. In this study, the effect of adding basalt fiber (BF), which is an inorganic fiber with high-temperature resistance for the production of ECC, was studied. Moreover, the change in the mechanical properties of ECC, including compressive, tensile, and flexural strength, was experimentally investigated under elevated temperatures up to 400 °C. The results showed that the addition of BF to reinforced ECC improved the tensile and flexural strength of concrete effectively, but compressive strength marginally decreased. A significant decrease was observed in the range from 300 to 400 °C, while it increased smoothly when heated up to 300 °C. The compressive and flexural strength diminished after a slight strain gained when heated up to 100 °C. This work paves the way for future investigations focusing on the development of high-temperature resistance ECC.

Keywords: engineered cementitious composites; basalt fiber; temperature; compressive strength; tensile strength; flexural strength

Citation: Rafiei, P.; Shokravi, H.; Mohammadyan-Yasouj, S.E.; Koloor, S.S.R.; Petrů, M. Temperature Impact on Engineered Cementitious Composite Containing Basalt Fibers. *Appl. Sci.* **2021**, *11*, 6848. https://doi.org/10.3390/app11156848

Academic Editor: Seong-Cheol Lee

Received: 25 June 2021
Accepted: 23 July 2021
Published: 26 July 2021

1. Introduction

Structures made of cementitious composites are widely constructed all around the world [1–3]. Achieving enhanced properties for cementitious composites in the fresh and hardened states could improve the performance of structures and reduce maintenance costs due to the fact of damages [4,5]. Engineered cementitious composite (ECC) is a new generation of high-performance fiber-reinforced cementitious composites characterized by high ductility, enhanced durability, and unique multiple fine cracking behaviors [6–8]. Engineered cementitious composite is generally composed of fine aggregates, admixtures, cement, additives, fibers, and water. Normally, ECC consists of well-graded, fine aggregate; therefore, no coarse aggregates are added to the matrix composition. Intrinsically, ordinary ECC is costly and has high energy and carbon footprints. A straightforward approach to this problem is partial or total replacement of cement and/or fine aggregates with other low-cost alternatives such as fly ash [9–11], ground granulated blast-furnace slag [12–14], and coarse sands [15–17].

Engineered cementitious composite was developed by Li et al. [18–20] based on fracture mechanic principles to serve multiple cracking properties and pseudo strain-hardening. Theoretically, strain-hardening in ECC is measured by two performance indices: the energy

performance index and the stress performance index [21,22]. The stress performance index first involves cracking strength and is defined as the ratio of the tensile strength of the composite to the initial cracking strength. Both the energy and stress performance indices must be larger than the unity to ensure multiple cracking behavior [23]. Fibers have a very important role in the crack bridging action of ECC composites, and fiber rupture depends on fiber strength and their chemical bonding within the concrete matrix [24]. To study the chemical bonding of the fibers within the composite medium, microstructural and micromechanical properties of ECC are generally evaluated using SEM and AFM [25], X-ray micro-computed tomography (μCT) [26], and the single-fiber pullout test [25,27].

Traditional ECC materials contain polyvinyl-alcohol (PVA) fibers known as PVA-ECC, while other fibers with inorganic (e.g., carbon, steel, glass, and basalt fibers), polymeric (e.g., polypropylene (PP), polyester, polyethylene (PE), and nylon) nature and natural fibers (e.g., silk, wool, asbestos, wollastonites, coir, cotton, and sisal) have recently been used widely [28–30]. Polyvinyl-alcohol fibers exhibited better and more consistent ductility improvement compared to other types of fibers. Polypropylene fiber is softer, cheaper, and it disperses faster compared to PVA or PE fibers, which results in better workability of the fresh composite [31]. Moreover, PP fiber has better durability when exposed to an alkaline environment due to the fact of its hydrophobic and non-polar nature [32]. Despite the advantages offered by adding fibers in ECC compositions, some drawbacks, such as a reduction in compressive strength, and an increase in shrinkage and porosity were reported for excess use of fibers [33]. Virgin PE fiber has low mechanical bonds, and they are vulnerable to degradation in the alkaline concrete environment [34–36]. Hence, some interface modifications and surface treatment are required to improve fiber/matrix bonding and stability [36]. Natural fibers, particularly those with plant origin, show good promise in improving flexural performance and reducing shrinkage. However, natural fibers are generally of very restricted durability which limits their utilization. Man-made fibers, such as steel and carbon fibers, are found more commonly in conventional ECC. Among all, basalt fiber (BF) attracts significant attention due to the abundance of basalt resources and low cost and low carbon and energy footprints during manufacturing [36].

Engineered cementitious composite can be classified as a high-performance fiber-reinforced cementitious composite with a ductility that ranges from 3% to 5% of strain having 1.5–2% fiber content by volume [18–20]. The incorporation of fibers in ECC composites increases ductility and delays the growth of small cracks so as to improving the post-crack behavior [37,38]. Engineered cementitious composite is characterized by moderate tensile strength ranging from 4 to 6 MPa. However, ECC shows a strain-hardening behavior after the initial matrix cracking, leading to the development of high tensile ductility in the range of 3–7% [39]. Though the compressive strength of ECC is almost equivalent to that of normal Portland concrete, the elastic modulus of ECC is smaller due to the absence of coarse aggregate. The induced tensile load on ECC composite elements allows for the formation of multiple cracks, with a small opening of an individual crack having widths below 50 μm [40]. The formation of small cracks improves resistance to water permeability and chloride diffusivity [41,42]. Hence, ECC materials have great potential for application in concrete structures exposed to a corrosive environment [43–45].

The ECC can considerably improve the structural performance of reinforced concrete elements. Li et al. [46] studied the flexural capacities of pre-cast ECC panels in permanent formworks. The results of the bending test showed significant improvement in the load capacity and toughness of a concrete member and effective dispersing of a single crack into multiple ones in ECC. Zhang et al. [47] investigated the shear behavior of ECC permanent formwork. It was shown that using ECC permanent formwork could significantly enhance the deformation and shear carrying capacity of reinforced concrete (RC) slender beams without stirrups. Pan et al. [48] investigated the failure pattern and seismic behavior of the ECC column using quasi-static tests. The result of experimental research indicated the better seismic performance of reinforced ECC composite columns compared to normal RC columns. Significant enhancement in seismic performance in terms of energy dissipa-

tion capacity, ductility, and damage tolerance was reported. Qiao et al. [49] presented a nonlinear analysis to study the flexural behavior of an ECC beam and the bilateral interaction of flexural behavior and the applied interface treatments on enhancing the element's durability.

The demand for ECC composites for different technical and operational conditions led to the development of different matrices with special fresh and hardened attributes. Self-compacting (SC) [50], high-early-strength (HES) [51], self-healing (SH) [52], green (G) [53], and lightweight (LW) [54] engineered cementitious composites are the most widely studied ECC composites in the literature. Lightweight ECC is defined as cementitious composites made with a variety of low-density ingredients including entrained air, shale, hollow glass bubbles, and polymeric beads [55]. However, the ECC achieved by low-density ingredients often results in brittleness and reduction in tensile and compressive strengths [55]. HES-ECC is developed to address the need for concrete repair applications in which minimum operations disruption is desired [56]. The compressive strength of 17.2 MPa at 4 h is the minimum targeted early strength of ECC based on the requirements of the Federal Highway Administration (FHWA) and Department of Transportation (DOT) that is set for after placement reopening of transportation to traffic [55].

Maalej and Li [57], in one of the first studies on ECC, researched strain-hardening behavior and crack propagation. It was concluded that the crack control in ECC was better than in fiber concrete. Lee et al. [58] used PE fibers in ECC composites and showed that these fibers could significantly increase the tensile and flexural strength of ECC. Kanda and Lee [21] used PVA fibers to produce ECC that was more environmentally friendly. Singh et al. [59] investigated the effects of hybrid addition of steel–PE fibers on the compressive and flexural strength and stiffness of fiber hybrid-reinforced concrete. It was observed that the best performance was achieved with the ratio 75% steel fibers and 25% polypropylene fibers. Fischer [60] conducted an experimental study to compare the deformation behavior of reinforced ECC flexural members under cyclic load. No cracks were observed in the columns containing ECC under the applied load. Said and Razak [61] reported that the addition of polyethylene fibers reduced the compressive strength due to the uneven fiber distribution, while the strain and tensibility of the composite were improved.

Singh and Munjal [62] conducted a comparative study on the mechanical properties of PVA and polyester fibers in ECC composites. It was concluded that ECC containing PVA fibers had a higher tensile, compressive, and flexural strength compared to ECC containing polyester fibers. Kang [62] carried out an experimental investigation on the shear strength of ECC and showed that the shear strength was higher due to the presence of these fibers in ECC containing fly ash and ground granulated blast-furnace slag. Sui et al. [63] investigated the bond behavior in FRP–ECC–concrete interfaces. It was concluded that the addition of an ECC layer could significantly enhance the maximum strain of FRP and delay the debonding failure. The other interface characteristics of the contact surface, such as bearing capacity, the ultimate slip, and the interface energy consumption capacity, were also improved. Ammasi et al. [64] carried out an experimental study to explore the effect of partial (i.e., 40%, 60%, 80%) and total replacement of cement content in ECC with fly ash on mechanical properties such as compressive strength, flexural strength, splitting tensile strength, and modulus of elasticity. In the partial replacement of fly ash, from 40% to 60%, an improvement was observed in the mechanical properties. Similarly, the chloride ion penetration was significantly decreased by the increase in fly ash content from 40% to 100%.

Temperature has a significant effect on the mechanical properties of the hardened cementitious composites [65]. Yu et al. [66] studied the performance of ECC containing a very high volume of fly ash, and PVA fibers were exposed to 20 °C, 50 °C, 100 °C, and 200 °C. Nonetheless, the melting temperature of PVA fibers was approximately 230 °C, and the mechanical properties were enhanced from 50 to 100 °C. The tensile properties diminished after exposure to 200 °C.

Bhat et al. [67] discussed the effect of elevated temperature levels up to 600 °C on the strain-hardening of ECC. The ECC demonstrated high spalling resistance after 6 h of exposure to 600 °C. Du et al. [68] evaluated the effects of high temperature on compressive strength, modulus of elasticity, compressive strain capacity, and flexural strength of PVA-ECC subjected to 20 °C, 100 °C, 200 °C, 300 °C, and 400 °C for 6 h. Temperature increase diminished the compressive strength, modulus of elasticity, and flexural strength. The compressive strain capacity was significantly enhanced under elevated temperatures. Xu et al. [69] investigated the strain-hardening and multiple cracking behavior of BF-reinforced ECC (BF-ECC) considering the bridging action of BFs.

There exists a large body of literature to study the BF-ECC under ambient or extreme environmental conditions. Xu et al. [69] studied the mechanical properties of BF-ECC under ambient temperature. Wu et al. [70] investigated the effect of salt freeze–thaw cycles on BE-ECC and its interface with concrete. Singh et al. [71] analyzed the effect of the composition of ECC on its performance under ambient temperature. Despite this, relatively little is known about the performance of BF-ECC exposed to elevated temperatures. This research aimed to study the effect of adding BF for the production of ECC under elevated temperatures up to 400 °C. Moreover, the change in the mechanical properties of ECC, including compressive, tensile, and flexural strength, was experimentally investigated. In the first step, the control mix was designed. In the next phase, several matrices with different amounts of BF and matrix ingredients were designed. Compressive, tensile, and flexural tests were carried out to characterize the macro-scale mechanical behaviors. The focus of the present research was on the development of BF-ECC. The performance of BF-ECC at elevated temperatures, however, may remain an interesting matter for future investigations.

2. Materials and Methods

2.1. Materials

The materials used in this experimental study for the production of ECC mixtures were Type I ordinary Portland cement (Sepahan Co.) complying with the requirements of the ASTM C150 standard, fine silica sand, class F normal fly ash complying with ASTM C618 requirements, BFs with a 10 mm average length and 20–13 μm in diameter, water, and superplasticizer to improve workability, which were all purchased or provided from local suppliers. Fine silica sand is the standard aggregate in ECC to achieve even dispersion of fibers and plane cracking pattern, while limited studies have used coarser sand [72,73]. Around three-quarters of the composite's volume were occupied by aggregates. Hence, their quality and composition may adversely affect the durability and structural behavior of the hardened composite. The physical and chemical properties of the used fine aggregate are shown in Table 1. Fine silica sand with a maximum grain size of 180 μm and an average grain size of 100 μm was used as filler and aggregate.

Table 1. Chemical properties of fine silica sand used in this study.

pH	Solubility	Moisture	Fluoride (PPM)	Calcium	Phosphorous
4–7	Minimum 85%	Maximum 3%	Maximum s1800	Minimum 21%	Minimum 17%

Adding BFs into ECC enhances the mechanical properties and reduces its brittleness. Unlike other fibers, such as steel or polypropylene, BFs are formed in the manufacturing industry in bundles and cut into required lengths. However, the chopped BFs do not have a uniform length and diameter as shown in Figure 1. It is normal to consider the average diameter and length of BFs that are introduced by the provided datasheet from the manufacturer [5,74,75]. The mechanical properties of the BFs supplied by the manufacturer are shown in Table 2.

Table 2. Mechanical characteristics of basalt fiber (BF).

Length of Fiber (mm)	Equivalent Diameter (µm)	Water Absorption(%)	Tensile Strength (N/mm^2)	Melting Point (C·)	Elastic Modulus (GPa)	Ultimate Elongation (%)
10	13–20	<0.5	4100–4800	1050	93–110	1.3–3.2

Figure 1. The basalt fibers (BFs) used in the production of the ECC mixture.

2.2. Mix Designs and Preparation of Specimens

The geometrical characteristics and volume fraction of the chopped fibers and matrix rheology are among the most important parameters in the mix design that may strongly affect the fiber distribution in the ECC matrix [76]. The parameter for fiber volume fraction has been widely examined in the studies presented in the literature review. The amount of BF content in ECC mixes in the previous studies generally ranged from 1% to 5% of the total ECC volume. However, the findings in these studies suggest using a fiber volume fraction of 2.5%. Based on the literature, fibers with shorter lengths have shown better distribution, while the longer length of chopped BFs provides a more efficient crack-bridging ability. Hence, an average length of 10 mm was selected for the utilized BFs, which is consistent with the literature. To determine the proportions of cementitious composite, in the experimental study, a base mix was designed to achieve a target 28 day cylinder compressive strength of 40 MPa. For the control mix, the proportioning of the ingredients is as per Table 3.

Table 3. The mix design and the proportions of the constituent materials in the ECC.

Concrete Type	Cement (kg/m^3)	Silica Sand (kg/m^3)	Fly Ash (kg/m^3)	Water (kg/m^3)	Superplasticizer (kg/m^3)	BFs (%)
Reference mix (R-ECC)	820	656	205	379		-
BF-ECC	820	656	205	379	8.74	2.5

The mix proportion of the BF-ECC in this experiment was the same as the mix design as the reference mix, while the BF and superplasticizer contained 2.5% of the volume fraction and 7.84 (kg/m^3) of the ECC content, respectively. Water-reducing admixture was added to the ECC to obtain the same flow compared to the reference mixture. The utilized water-reducing admixture was a polycarboxylate-based superplasticizer with a specific gravity of 1.05 (g/m^3) and pH of 7. The ratios of the sand, fly ash, and water to cement in the reference and fiber-included mixes were 0.8, 0.25, and 0.37, respectively. Uniform fiber distribution is a crucial factor for enhanced mechanical properties, especially tensile strength and ductility in ECC [76]. Applying a correct mixing sequence of the material can enhance the mechanical properties and improve fiber distribution [77]. In the first step, the ingredients were weighed and prepared separately.

The equipment used for mixing ingredients was a rotary 60-L pan-type concrete mixture supplied with 220 V AC power and a frequency of 50 Hz. The mixing rotational speed of the mixture was around 35 rpm in compliance with EN 12390-2. In the first stage, the solid ingredients, including silica sand, cement, and fly ash were premixed in a mixing vessel with a nominal speed for a couple of minutes before liquid loading. At the same time, the superplasticizer was added to water and stirred for 2–3 min. Then, the liquid mixture was poured into the dry mixture and mixed for another 3 min in accordance with the procedure explained by Yang et al. [78]. The fibers were split into strands for a more even dispersion in the cementitious matrix and to prevent agglomeration. Then the well-separated fibers were uniformly sprinkled into the cementitious composite while the stirring mill was working at normal speed for 3 min. Typically, an even fiber distribution and proper consistency of the cementitious mortar can be achieved after 3 min of mixing time advised by Li et al. [79] and Fischer et al. [80]. The mix of composition continued for 7 min at normal speed to ensure an even distribution of the chopped fibers in the mixture.

The fresh ECC was poured into molds and compacted according to the ASTM standards. For each temperature exposure scenario (25 °C, 100 °C, 200 °C, 300 °C, and 400 °C), three cubic, cylindrical, and prismatical specimens were tested. The mixture was cast into metal cubic molds with the dimension of 50 mm × 50 mm × 50 mm for compressive strength test according to ASTMC109/C109M-08, metal cylindrical molds with the dimension of 200 mm × 100 mm for the split tensile test according to ASTM C496, and prismatic molds with the dimension of 40 mm × 40 mm × 160 mm for the three-point bending test according to ASTMC348-08. At the age of 28 days, the ECC specimens were placed and kept in an oven for temperature exposure scenarios. Triplicate specimens for each temperature range and strength test was tested. The molded specimens for compressive, split tensile, and flexural tests are shown in Figure 2.

Figure 2. Molds after casting for tensile, flexural, and compressive strength tests from top downward, respectively.

2.3. Mechanical Properties

Compressive, flexural, and tensile strength tests were carried out on specimens according to ASTM standards. Triplicate specimens for each batch and temperature range were prepared and tested. The average values of the triplicate specimens were taken as the representative results. The compressive strength tests were performed on 50 mm cube ECC specimens conforming to ASTM C109-08. A compression machine with 2000 kN capacity was used to determine the ultimate load-carrying capacity of the ECC specimens under pure compression. An axial compressive load was applied with a rate of 0.4 kN/s according to the ASTM C31 test method. The pressure was continued until the specimen was crushed. The failure point corresponded to the ultimate load- and stress-bearing capacity of specimens in kN and MPa, respectively. The splitting tensile test was carried out to assess the tensile bond strength of the ECC specimens. The same universal testing machine with a rate of 0.4 kN/s was used for splitting tensile tests according to ASTM C496. Prisms specimens with the dimension of 40 mm × 40 mm × 160 mm and curing age of 28 days were used for the flexural strength test. The test continued within a three-point loading arrangement until an audible and visible crack was observed. The hardened specimens were heated to three different temperatures of 100 °C, 200 °C, 300 °C, and 400 °C for a duration of 10 min after 28 days of curing. In order to prevent cooling shock, samples were left at room temperature to cool down gradually before applying compressive load in the testing machine. Figure 3 shows the testing machines used for flexural and compressive strength.

(**a**)

(**b**)

Figure 3. Testing machines used for (**a**) flexural strength and (**b**) compressive strength.

3. Result and Discussions

In this chapter, the results of experiments performed on the mechanical properties of fiber-free and fiber-reinforced ECC along with diagrams are presented and a comparison is made between them.

3.1. Results of the Compressive Strength Test

Compressive strength is the most important mechanical characteristic of construction materials due to the fact of its significant role as the compliance criteria in standards and specifications. The compressive strength of the cubic samples of 50 mm in dimension made according to the ASTM C109/C109 M-08 standard was first tested after 28 days of curing at room temperature without exposure to high temperatures. The compressive strength of the samples in fiber-reinforced and fiber-free specimens was 41.7 MPa and 43.3 MP, respectively. The results of the compressive strength tests are illustrated in Figure 4 for reference mixes and fiber-reinforced ECC. The results in each point were obtained from the average of triplicate specimens.

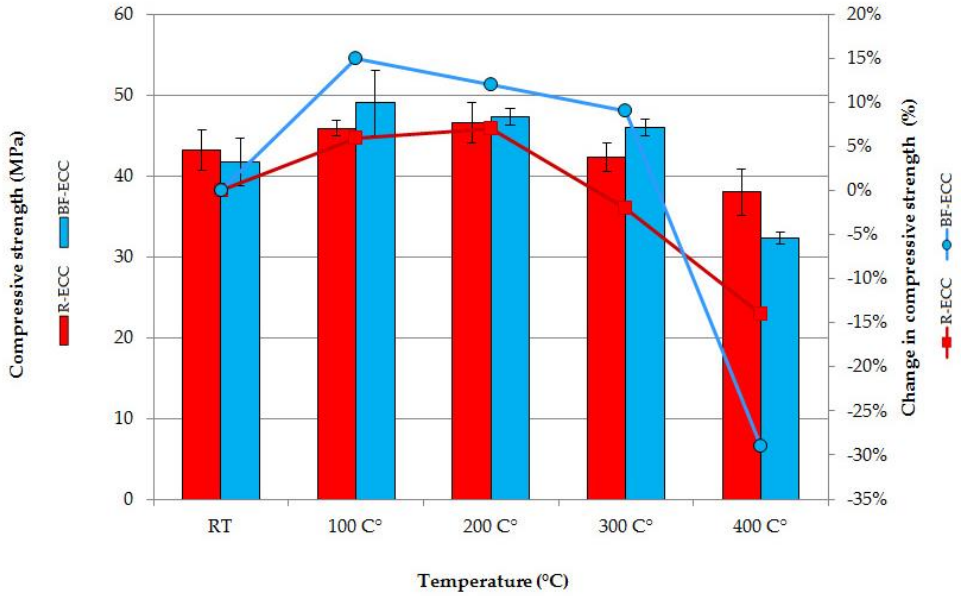

Figure 4. The result of the change in compressive strength of fiber-reinforced and fiber-free fibrous specimens exposed to elevated temperatures up to 400 °C.

It was observed that the temperature increase in BF-reinforced ECC up to 100 °C increased the compressive strength, while exposure to a higher temperature range (i.e., 100–400 °C) resulted in approximately 44% of its decrease. The maximum growth in the compressive strength of BF-ECC was achieved at 100 °C. With the passage of time, cement hydration increased. The encapsulated micro- or macro-size water droplets within the concrete composition were gradually released by temperature increases from room temperature to 100 °C. The evaporation of the encapsulated water improved the curing efficiency by facilitating the hydration of the cementitious system and positively influenced the strength growth rate of the concrete. The pattern of change in compressive strength of the BF-ECC was similar to the one for the reference state except in the range of 100–200 °C where there existed small increases in compressive strength in the reference ECC, while there was a decrement in the BF-ECC. However, the range of variation in the R-ECC was much smoother compared to the BF-ECC due to the fact of exposure to an elevated temperature. Reduction in the compressive strength of the ECC under an elevated temperature up to 400 °C may be due to the fact that this concrete completely lost its water up to 400 °C. Up to 100 °C, the hydration of waterless cement aggregates improved due to the fact of its internal autoclave conditions. This is especially the case with high-strength concrete. The above is true because its low permeability had a great effect on moisture transfer. In the temperatures above 350 °C, calcium hydroxide decomposed into either lime and water, or C–S–H due to the pozzolanic reaction accelerated at high temperatures, where the decomposition of hydroxide calcium had a minor effect on the reduction in resistance.

The reduction in the compressive strength by the addition of BF is in agreement with the experimental result observations reported by other authors [81–83]. This decrease was mainly caused by compactness reduction due to the introduction of voids into the ECC matrix during the incorporation of the BFs into the composite. However, the observation during compressive tests of BF-ECC indicated a more ductile failure absorbing a larger amount of plastic energy under compressive loads compared to the fiber-free control mixture.

3.2. Results of the Indirect Tensile Strength Test

A tensile test was performed to verify the crack opening performance under the complex stress state. The splitting tensile strength of the fiber-reinforced and control cylinder specimens was made according to the ASTM C496 standard. The specimens were

tested after exposure to five temperature conditions: room temperature, 100 °C, 200 °C, 300 °C, and 400 °C. The tensile strength of the BF-reinforced and control samples were 4.25 MPa and 3.1 MP, respectively. The results of the tensile strength tests, for the control and fiber-reinforced ECC mixes, are illustrated in Figure 5. The results in each point were obtained from the average of triplicate specimens.

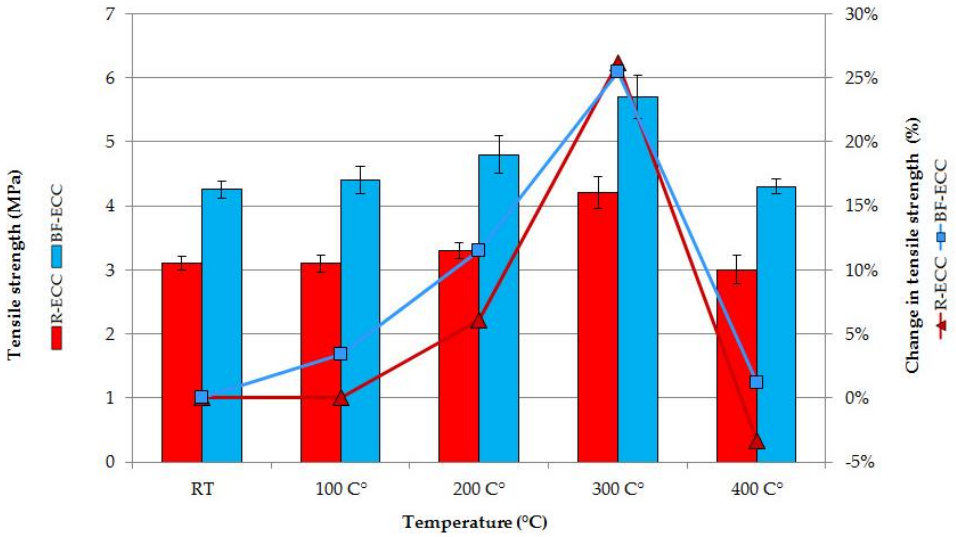

Figure 5. The result of the change in tensile strength of control and fiber-reinforced specimens exposed to elevated temperatures up to 400 °C.

Figure 5 shows that BF-reinforced ECC had a higher tensile strength than the control samples. Higher tensile strength was achieved due to the addition of fiber resulting in advantages such as an increased ductility, better crack resistance, and energy absorption capacity. With the increasing temperature up to 300 °C, the tensile strength increased, while a significant reduction in the strength capacity was recorded when the temperature was raised from 300 to 400 °C. Quite a similar pattern was observed for the tensile strength of control and BF-reinforced ECC. From the obtained results in Figures 4 and 5, it can be observed that the rate of increase in compressive strength and tensile strength due to the elevated temperature did not follow the same trend despite their correlation [84].

The results show that the tensile strength of samples containing BFs was higher than samples without fibers at all temperatures tested. In addition, the largest difference in tensile strength between the control and BF-reinforced samples was at 300 °C. The increase in the tensile strength of fiber-containing samples, compared to control ones, could be due to the phenomenon of fiber bridging and the combination and friction of fiber combinations. With increasing temperature up to 300 °C, hydration of waterless cement grains improved due to the internal autoclave conditions. No microcracks were observed in the interfacial transition zone (ITZ) of the ECC samples up to 200 °C. As the temperature rose to 400 °C, the width and length of microcracks were found to greatly increase in intensity. The reason for the formation of microcracks was that the cement composition shrunk with water loss, while the aggregates expanded due to increasing temperature resulting in crack generation in the ITZ.

3.3. Results of the Flexural Strength Test

Flexural strength is the bending property in a concrete beam under flexural loading. The flexural strength test at 28 days of ECC prism specimens was performed with a three-point loading configuration conforming to ASTM C348-08. The reinforcing effect of the BF on the flexural behavior of the ECC mix was specifically manifested by an increase in flexural strength. The test results showed that the compressive strength of the samples in BF-reinforced and controlled specimens was 10.4 MPa and 8.6 MP, respectively. The results

of the flexural strength tests are illustrated in Figure 6 for the control and BF-reinforced ECC mixes. The results in each point were calculated from the average of triplicate specimens.

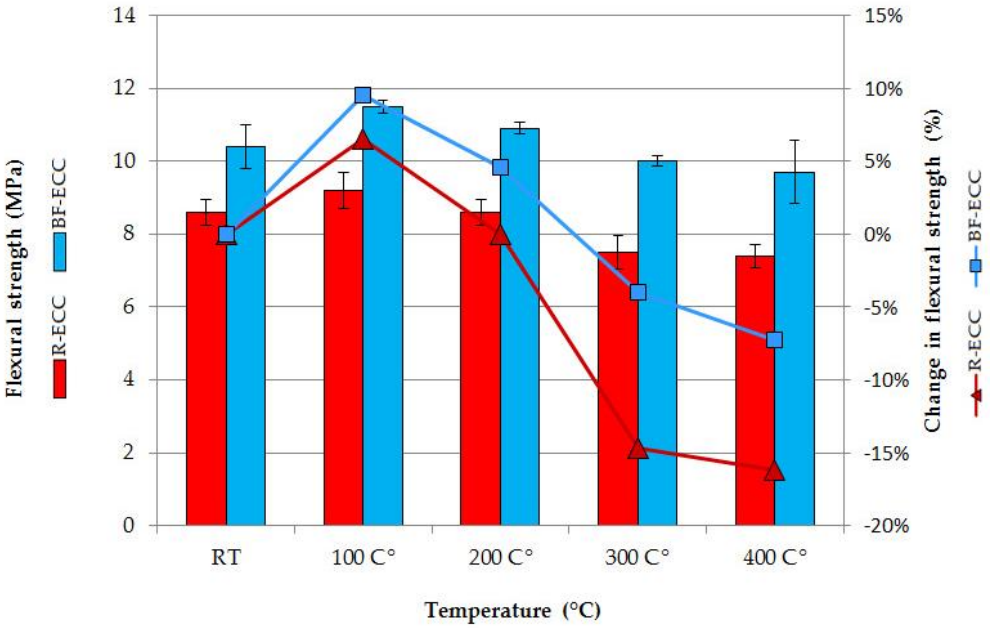

Figure 6. Comparing the splitting tensile strength test of the control and BF-containing samples under elevated temperatures.

It was observed that the increase in temperature in the BF-reinforced ECC up to 100 °C increased the tensile strength, while exposure to a higher temperature range (i.e., 100–400 °C) resulted in its decrease. The flexural strengths of the R-ECC and BF-ECC at 400 °C were 16% and 7% lower than those at room temperature. The maximum growth in the compressive strength of BF-ECC was achieved at 100 °C. The pattern of change in compressive strength of the BF-ECC was similar to the one for the reference state. However, the range of variation in R-ECC was much higher compared to BF-ECC due to the exposure to an elevated temperature. The rate of flexural strength development under elevated temperature in BF-ECC up to 100 °C temperature was 3% higher, while the strength loss from 100 to 400 °C was 9% lower compared to control specimens. Reduction in the tensile strength of the ECC under elevated temperature up to 400 °C may be due to the fact that this concrete completely lost its water up to 400 °C. Up to 100 °C, the hydration of cement was improved due to the internal autoclave conditions.

4. Conclusions

In this study, the compressive, tensile, and flexural strength of control and BF-ECC specimens were evaluated under elevated temperatures. Based on the research results stated earlier, adding BFs to the ECC did not have a significant effect on the compressive strength; however, there was a slight decrease in compressive strength of BF-ECC when exposed to the elevated temperature from 100 to 300 °C. The highest increment in compressive strength of the BF-ECC was achieved when the temperature was raised to 100 °C. The increment in this compressive strength might be due to the evaporation of the encapsulated water resulting in improving the curing efficiency strength growth rate of the concrete. Adding BFs to the ECC could significantly increase the tensile strength of the concrete in all tested temperatures. The highest tensile strength of these composites is at 300 °C. Abrupt loss of tensile strength is reported in the range of 300–400 °C. Adding BFs to the ECC increased the flexural strength before heating and after heating. In addition, the highest flexural strength of engineered cement composite was at a temperature of 300 °C. The addition of BFs to ECC could significantly increase the tensile and flexural strength of

ECC with and without heat exposure. This work paves the way for future investigations focusing on the development of high-temperature resistance ECC.

Author Contributions: Conceptualization, P.R. and S.E.M.-Y.; methodology, P.R. and S.E.M.-Y.; software, P.R., S.E.M.-Y. and H.S.; validation, P.R. and S.E.M.-Y.; formal analysis, P.R. and S.E.M.-Y.; investigation, P.R., S.E.M.-Y. and H.S.; resources, P.R., S.E.M.-Y., H.S., S.S.R.K. and M.P.; data curation, P.R.; writing—original draft preparation, H.S., S.E.M.-Y. and P.R.; writing—review and editing, H.S., S.E.M.-Y., P.R. and S.S.R.K.; visualization, P.R., S.E.M.-Y., H.S., S.S.R.K. and M.P.; supervision, S.E.M.-Y.; project administration, P.R., S.E.M.-Y., H.S., S.S.R.K. and M.P. funding acquisition, P.R., S.E.M.-Y., H.S., S.S.R.K. and M.P. All authors have read and agreed to the published version of the manuscript.

Funding: The research was funded and supported by Islamic Azad University, Najafabad Branch, and the Ministry of Education, Youth and Sports of the Czech Republic and the European Union (European Structural and Investment Funds–Operational Programme Research, Development and Education, Reg. No. CZ.02.1.01/0.0/0.0/16_025/0007293).

Institutional Review Board Statement: Not applicable.

Informed Consent Statement: Not applicable.

Data Availability Statement: Not applicable.

Conflicts of Interest: The authors declare no conflict of interest.

References

1. Shokravi, H.; Shokravi, H.; Bakhary, N.; Koloor, S.S.R.; Petrů, M. Health monitoring of civil infrastructures by Subspace system identification method: An overview. *Appl. Sci.* **2020**, *10*, 2786. [CrossRef]
2. Shokravi, H.; Shokravi, H.; Bakhary, N.; Heidarrezaei, M.; Rahimian Koloor, S.S.; Petrů, M. Application of the subspace-based methods in health monitoring of civil structures: A systematic review and meta-analysis. *Appl. Sci.* **2020**, *10*, 3607. [CrossRef]
3. Shokravi, H.; Shokravi, H.; Bakhary, N.; Koloor, S.S.R.; Petrů, M. A comparative study of the data-driven stochastic subspace methods for health monitoring of structures: A bridge case study. *Appl. Sci.* **2020**, *10*, 3132. [CrossRef]
4. Shokravi, H.; Shokravi, H.; Bakhary, N.; Heidarrezaei, M.; Koloor, S.S.R.; Petru, M. Vehicle-assisted techniques for health monitoring of bridges. *Sensors* **2020**, *20*, 3460. [CrossRef]
5. Mohammadyan-Yasouj, S.E.; Ahangar, H.A.; Oskoei, N.A.; Shokravi, H.; Koloor, S.S.R.; Petrů, M. Thermal performance of alginate concrete reinforced with basalt fiber. *Crystals* **2020**, *10*, 779. [CrossRef]
6. Pan, Z.; Wu, C.; Liu, J.; Wang, W.; Liu, J. Study on mechanical properties of cost-effective polyvinyl alcohol engineered cementitious composites (PVA-ECC). *Constr. Build. Mater.* **2015**, *78*, 397–404. [CrossRef]
7. Luković, M.; Hordijk, D.A.; Huang, Z.; Schlangen, E. Strain Hardening Cementitious Composite (SHCC) for crack width control in reinforced concrete beams. *Heron* **2019**, *64*, 181.
8. Zhang, R.; Meng, Q.; Shui, Q.; He, W.; Chen, K.; Liang, M.; Sun, Z. Cyclic response of RC composite bridge columns with precast PP-ECC jackets in the region of plastic hinges. *Compos. Struct.* **2019**, *221*, 110844. [CrossRef]
9. Nematollahi, B.; Sanjayan, J.; Ahmed Shaikh, F.U. Tensile strain hardening behavior of PVA fiber-reinforced engineered geopolymer composite. *J. Mater. Civ. Eng.* **2015**, *27*, 4015001. [CrossRef]
10. Yu, J.; Leung, C.K.Y. Strength improvement of strain-hardening cementitious composites with ultrahigh-volume fly ash. *J. Mater. Civ. Eng.* **2017**, *29*, 5017003. [CrossRef]
11. Ohno, M.; Li, V.C. A feasibility study of strain hardening fiber reinforced fly ash-based geopolymer composites. *Constr. Build. Mater.* **2014**, *57*, 163–168. [CrossRef]
12. Zhou, J.; Qian, S.; Beltran, M.G.S.; Ye, G.; van Breugel, K.; Li, V.C. Development of engineered cementitious composites with limestone powder and blast furnace slag. *Mater. Struct.* **2010**, *43*, 803–814. [CrossRef]
13. Chen, Z.; Yang, Y.; Yao, Y. Quasi-static and dynamic compressive mechanical properties of engineered cementitious composite incorporating ground granulated blast furnace slag. *Mater. Des.* **2013**, *44*, 500–508. [CrossRef]
14. Qiu, J.; Tan, H.S.; Yang, E.-H. Coupled effects of crack width, slag content, and conditioning alkalinity on autogenous healing of engineered cementitious composites. *Cem. Concr. Compos.* **2016**, *73*, 203–212. [CrossRef]
15. Paul, S.C.; van Zijl, G.P.A.G. Mechanically induced cracking behaviour in fine and coarse sand strain hardening cement based composites (SHCC) at different load levels. *J. Adv. Concr. Technol.* **2013**, *11*, 301–311. [CrossRef]
16. Sahmaran, M.; Lachemi, M.; Hossain, K.M.A.; Ranade, R.; Li, V.C. Influence of aggregate type and size on ductility and mechanical properties of engineered cementitious composites. *ACI Mater. J.* **2009**, *106*, 308.
17. Choi, W.-C.; Yun, H.-D.; Kang, J.-W.; Kim, S.-W. Development of recycled strain-hardening cement-based composite (SHCC) for sustainable infrastructures. *Compos. Part B Eng.* **2012**, *43*, 627–635. [CrossRef]
18. Li, V.C. Engineered Cementitious Composites (ECC)-Tailored Composites Through Micromechanical Modeling. *J. Adv. Concr. Technol.* **1998**. [CrossRef]

19. Li, V.C.; Stang, H.; Krenchel, H. Micromechanics of crack bridging in fibre-reinforced concrete. *Mater. Struct.* **1993**, *26*, 486–494. [CrossRef]
20. Li, V.C.; Leung, C.K.Y. Steady-state and multiple cracking of short random fiber composites. *J. Eng. Mech.* **1992**, *118*, 2246–2264. [CrossRef]
21. Kanda, T.; Li, V.C. Interface property and apparent strength of high-strength hydrophilic fiber in cement matrix. *J. Mater. Civ. Eng.* **1998**, *10*, 5–13. [CrossRef]
22. Kanda, T.; Li, V.C. Multiple cracking sequence and saturation in fiber reinforced cementitious composites. *Concr. Res. Technol.* **1998**, *9*, 19–33. [CrossRef]
23. Hyun, J.H.; Lee, B.Y.; Kim, Y.Y. Composite properties and micromechanical analysis of highly ductile cement composite incorporating limestone powder. *Appl. Sci.* **2018**, *8*, 151. [CrossRef]
24. Kanda, T.; Li, V.C. Practical design criteria for saturated pseudo strain hardening behavior in ECC. *J. Adv. Concr. Technol.* **2006**, *4*, 59–72. [CrossRef]
25. Ding, C.; Guo, L.; Chen, B.; Xu, Y.; Cao, Y.; Fei, C. Micromechanics theory guidelines and method exploration for surface treatment of PVA fibers used in high-ductility cementitious composites. *Constr. Build. Mater.* **2019**, *196*, 154–165. [CrossRef]
26. Lu, C.; Li, V.C.; Leung, C.K.Y. Flaw characterization and correlation with cracking strength in Engineered Cementitious Composites (ECC). *Cem. Concr. Res.* **2018**, *107*, 64–74. [CrossRef]
27. Nematollahi, B.; Qiu, J.; Yang, E.-H.; Sanjayan, J. Micromechanics constitutive modelling and optimization of strain hardening geopolymer composite. *Ceram. Int.* **2017**, *43*, 5999–6007. [CrossRef]
28. da Costa, F.B.P.; Righi, D.P.; Graeff, A.G.; da Silva Filho, L.C.P. Experimental study of some durability properties of ECC with a more environmentally sustainable rice husk ash and high tenacity polypropylene fibers. *Constr. Build. Mater.* **2019**, *213*, 505–513. [CrossRef]
29. Halvaei, M.; Jamshidi, M.; Latifi, M. Application of low modulus polymeric fibers in engineered cementitious composites. *J. Ind. Text.* **2014**, *43*, 511–524. [CrossRef]
30. Said, S.H.; Razak, H.A.; Othman, I. Strength and deformation characteristics of engineered cementitious composite slabs with different polymer fibres. *J. Reinf. Plast. Compos.* **2015**, *34*, 1950–1962. [CrossRef]
31. Zhang, R.; Matsumoto, K.; Hirata, T.; Ishizeki, Y.; Niwa, J. Application of PP-ECC in beam–column joint connections of rigid-framed railway bridges to reduce transverse reinforcements. *Eng. Struct.* **2015**, *86*, 146–156. [CrossRef]
32. Brown, R.; Shukla, A.; Natarajan, K.R. *Fiber Reinforcement of Concrete Structures*; Dept. of Chemical Engineering, University of Rhode Island: Kingston, RI, USA, 2002.
33. Bahraq, A.A.; Maslehuddin, M.; Al-Dulaijan, S.U. Macro-and Micro-Properties of Engineered Cementitious Composites (ECCs) incorporating industrial waste materials: A review. *Arab. J. Sci. Eng.* **2020**, *45*, 1–27. [CrossRef]
34. Silva, D.A.D.; Betioli, A.M.; Gleize, P.J.P.; Roman, H.R.; Gomez, L.A.; Ribeiro, J.L.D. Degradation of recycled PET fibers in Portland cement-based materials. *Cem. Concr. Res.* **2005**, *35*, 1741–1746. [CrossRef]
35. Machovic, V.; Andertova, J.; Kopecky, L.; Cerny, M.; Borecka, L.; Pribyl, O.; Kolar, F.; Svitilova, J. Effect of aging of PET fibre on the mechanical properties of PET fibre reinforced cement composite. *Ceram. Silik.* **2008**, *52*, 172–182.
36. Zhang, D.; Yu, J.; Wu, H.; Jaworska, B.; Ellis, B.R.; Li, V.C. Discontinuous micro-fibers as intrinsic reinforcement for ductile Engineered Cementitious Composites (ECC). *Compos. Part B Eng.* **2020**, *184*, 107741. [CrossRef]
37. Leung, C.K.Y.; Cheung, Y.N.; Zhang, J. Fatigue enhancement of concrete beam with ECC layer. *Cem. Concr. Res.* **2007**, *37*, 743–750. [CrossRef]
38. Meghwar, S.L.; Khaskheli, G.B.; Kumar, A. Human scalp hair as fiber reinforcement in cement concrete. *Mehran Univ. Res. J. Eng. Technol.* **2020**, *39*, 443. [CrossRef]
39. Zhou, J.; Qian, S.; Ye, G.; Copuroglu, O.; van Breugel, K.; Li, V.C. Improved fiber distribution and mechanical properties of engineered cementitious composites by adjusting the mixing sequence. *Cem. Concr. Compos.* **2012**, *34*, 342–348. [CrossRef]
40. Huang, B.-T.; Li, Q.-H.; Xu, S.-L.; Li, C.-F. Development of reinforced ultra-high toughness cementitious composite permanent formwork: Experimental study and Digital Image Correlation analysis. *Compos. Struct.* **2017**, *180*, 892–903. [CrossRef]
41. Wang, K.; Jansen, D.C.; Shah, S.P.; Karr, A.F. Permeability study of cracked concrete. *Cem. Concr. Res.* **1997**, *27*, 381. [CrossRef]
42. Takewaka, K.; Yamaguchi, T.; Maeda, S. Simulation model for deterioration of concrete structures due to chloride attack. *J. Adv. Concr. Technol.* **2003**, *1*, 139–146. [CrossRef]
43. Şahmaran, M.; Li, V.C. Durability of mechanically loaded engineered cementitious composites under highly alkaline environments. *Cem. Concr. Compos.* **2008**, *30*, 72–81. [CrossRef]
44. Xinhua, X.S.C. Corrosion resistance of reinforced concrete beams with cover replaced by UHTCC. *China Civ. Eng. J.* **2011**, *5*, 2541.
45. Maalej, M.; Ahmed, S.F.U.; Paramasivam, P. Corrosion durability and structural response of functionally-graded concrete beams. *J. Adv. Concr. Technol.* **2003**, *1*, 307–316. [CrossRef]
46. Li, H.; Leung, C.K.Y.; Xu, S.; Cao, Q. Potential use of strain hardening ECC in permanent formwork with small scale flexural beams. *J. Wuhan Univ. Technol. Sci. Ed.* **2009**, *24*, 482–487. [CrossRef]
47. Zhang, R.; Hu, P.; Zheng, X.; Cai, L.; Guo, R.; Wei, D. Shear behavior of RC slender beams without stirrups by using precast U-shaped ECC permanent formwork. *Constr. Build. Mater.* **2020**, *260*, 120430. [CrossRef]
48. Pan, Z.; Liu, J.; Wu, C.; Qiao, Z.; Leung, C.; Meng, S. Experimental study and finite element analysis of seismic behavior of reinforced ECC composite columns. *J. Build. Struct.* **2017**, *38*, 38–45.

49. Qiao, Z.; Pan, Z.; Leung, C.K.Y.; Meng, S. Experimental study and analysis of flexural behavior of ECC/RC composite beams. *J. Southeast Univ.* **2017**, *47*, 724–731.
50. Thanh, H.T.; Li, J.; Zhang, Y.X. Numerical simulation of self-consolidating engineered cementitious composite flow with the V-funnel and U-box. *Constr. Build. Mater.* **2020**, *236*, 117467. [CrossRef]
51. Şahmaran, M.; Al-Emam, M.; Yıldırım, G.; Şimşek, Y.E.; Erdem, T.K.; Lachemi, M. High-early-strength ductile cementitious composites with characteristics of low early-age shrinkage for repair of infrastructures. *Mater. Struct. Constr.* **2015**, *48*, 1389–1403. [CrossRef]
52. Guan, X.; Zhang, C.; Li, Y.; Zhao, S. Effect of exposure conditions on self-healing behavior of engineered cementitious composite incorporating limestone powder. *Cem. Concr. Compos.* **2020**, *114*, 103808. [CrossRef]
53. Guo, M.; Zhong, Q.; Zhou, Y.; Hu, B.; Huang, Z.; Yue, Y. Influence of flexural loading and chloride exposure on the fatigue behavior of high-performance lightweight engineered cementitious composites. *Constr. Build. Mater.* **2020**, *249*, 118512. [CrossRef]
54. Xi, B.; Zhou, Y.; Yu, K.; Hu, B.; Huang, X.; Sui, L.; Xing, F. Use of nano-SiO_2 to develop a high performance green lightweight engineered cementitious composites containing fly ash cenospheres. *J. Clean. Prod.* **2020**, *262*, 121274. [CrossRef]
55. Li, V.C. Tailoring ECC for special attributes: A review. *Int. J. Concr. Struct. Mater.* **2012**, *6*, 135–144. [CrossRef]
56. Li, M.; Li, V.C. High-early-strength engineered cementitious composites for fast, durable concrete repair-material properties. *ACI Mater. J.* **2011**, *108*, 3.
57. Maalej, M.; Li, V.C. Flexural/tensile-strength ratio in engineered cementitious composites. *J. Mater. Civ. Eng.* **1994**, *6*, 513–528. [CrossRef]
58. Lee, B.Y.; Kim, J.-K.; Kim, Y.Y. Prediction of ECC tensile stress-strain curves based on modified fiber bridging relations considering fiber distribution characteristics. *Comput. Concr.* **2010**, *7*, 455–468. [CrossRef]
59. Singh, S.P.; Singh, A.P.; Bajaj, V. Strength and flexural toughness of concrete reinforced with steel-polypropylene hybrid fibres. *Asian J. Civ. Eng (Build. Hous.)* **2010**, *11*, 495–507.
60. Fischer, G.D. *Deformation Behavior of Reinforced ECC Flexural Members under Reversed Cyclic Loading Conditions*; University of Michigan: Ann Arbor, MI, USA, 2002; ISBN 049355646X.
61. Said, S.H.; Razak, H.A. The effect of synthetic polyethylene fiber on the strain hardening behavior of engineered cementitious composite (ECC). *Mater. Des.* **2015**, *86*, 447–457. [CrossRef]
62. Singh, S.B.; Munjal, P. Mechanical properties of PVA and polyester fibers based engineered cementitious composites. In *Recent Advances in Structural Engineering*; Springer: Berlin, Germany, 2019; Volume 1; pp. 715–728.
63. Sui, L.; Luo, M.; Yu, K.; Xing, F.; Li, P.; Zhou, Y.; Chen, C. Effect of engineered cementitious composite on the bond behavior between fiber-reinforced polymer and concrete. *Compos. Struct.* **2018**, *184*, 775–788. [CrossRef]
64. Ammasi, A.K. Strength and durability of high volume fly ash in engineered cementitious composites. *Mater. Today Proc.* **2018**, *5*, 24050–24058. [CrossRef]
65. Mohammadyan-Yasouj, S.E.; Heidari, N.; Shokravi, H. Influence of waste alumina powder on self-compacting concrete resistance under elevated temperature. *J. Build. Eng.* **2021**, *41*, 102360. [CrossRef]
66. Yu, J.; Lin, J.; Zhang, Z.; Li, V.C. Mechanical performance of ECC with high-volume fly ash after sub-elevated temperatures. *Constr. Build. Mater.* **2015**, *99*, 82–89. [CrossRef]
67. Bhat, P.S.; Chang, V.; Li, M. Effect of elevated temperature on strain-hardening engineered cementitious composites. *Constr. Build. Mater.* **2014**, *69*, 370–380. [CrossRef]
68. Du, Q.; Wei, J.; Lv, J. Effects of high temperature on mechanical properties of polyvinyl alcohol engineered cementitious composites (PVA-ECC). *Int. J. Civ. Eng.* **2018**, *16*, 965–972. [CrossRef]
69. Xu, M.; Song, S.; Feng, L.; Zhou, J.; Li, H.; Li, V.C. Development of basalt fiber engineered cementitious composites and its mechanical properties. *Constr. Build. Mater.* **2021**, *266*, 121173. [CrossRef]
70. Wu, X.; Tian, J.; Ma, H.; Zheng, Y.; Hu, S.; Wang, W.; Du, Y.; Huang, W.; Sun, C.; Zhu, Z. Investigation on interface fracture properties and nonlinear fracture model between ECC and concrete subjected to salt freeze-thaw cycles. *Constr. Build. Mater.* **2020**, *259*, 119785. [CrossRef]
71. Singh, M.; Saini, B.; Chalak, H.D. Performance and composition analysis of engineered cementitious composite (ECC)–A review. *J. Build. Eng.* **2019**, *26*, 100851. [CrossRef]
72. Wu, H.-L.; Yu, J.; Zhang, D.; Zheng, J.-X.; Li, V.C. Effect of morphological parameters of natural sand on mechanical properties of engineered cementitious composites. *Cem. Concr. Compos.* **2019**, *100*, 108–119. [CrossRef]
73. Zhang, Z.; Hu, J.; Ma, H. Feasibility study of ECC with self-healing capacity applied on the long-span steel bridge deck overlay. *Int. J. Pavement Eng.* **2019**, *20*, 884–893. [CrossRef]
74. Shokravi, H.; Mohammadyan-Yasouj, S.E.; Rahimian Koloor, S.S.; Petrů, M.; Heidarrezaei, M. Effect of alumina additives on mechanical and fresh properties of self-compacting concrete: A review. *Processes* **2021**, *9*, 554. [CrossRef]
75. Mohammadyan-Yasouj, S.E.; Ahangar, H.A.; Oskoei, N.A.; Shokravi, H.; Koloor, S.S.; Petrů, M. Experimental Study on the Effect of Basalt Fiber and Sodium Alginate in Polymer Concrete Exposed to Elevated Temperature. *Processes* **2021**, *9*, 510. [CrossRef]
76. Torigoe, S.; Horikoshi, T.; Ogawa, A.; Saito, T.; Hamada, T. Study on evaluation method for PVA fiber distribution in engineered cementitious composite. *J. Adv. Concr. Technol.* **2003**, *1*, 265–268. [CrossRef]
77. Niu, H.M.; Xing, Y.M.; Zhao, Y.R. A review on the methods of improving fiber distribution of engineered cementitious composites (ECC). In *Advanced Materials Research*; Trans Tech Publ: Zurich, Switzerland, 2013; Volume 683, pp. 46–50.

78. Yang, E.-H.; Yang, Y.; Li, V.C. Use of high volumes of fly ash to improve ECC mechanical properties and material greenness. *ACI Mater. J.* **2007**, *104*, 620.
79. Li, X.; Yang, X.; Ding, Z.; Du, X.; Wen, J. ECC design based on uniform design test method and alternating conditional expectation. *Math. Probl. Eng.* **2019**, *2019*, 1–14. [CrossRef]
80. FISCHER, G.; Shuxin, W. Design of engineered cementitious composites (ECC) for processing and workability requirements. In *Brittle Matrix Composites 7*; Elsevier: Amsterdam, The Netherlands, 2003; pp. 29–36.
81. Kabay, N. Abrasion resistance and fracture energy of concretes with basalt fiber. *Constr. Build. Mater.* **2014**, *50*, 95–101. [CrossRef]
82. Ayub, T.; Shafiq, N.; Nuruddin, M.F. Mechanical properties of high-performance concrete reinforced with basalt fibers. *Procedia Eng.* **2014**, *77*, 131–139. [CrossRef]
83. Sun, X.; Gao, Z.; Cao, P.; Zhou, C. Mechanical properties tests and multiscale numerical simulations for basalt fiber reinforced concrete. *Constr. Build. Mater.* **2019**, *202*, 58–72. [CrossRef]
84. Badarloo, B.; Kari, A.; Jafari, F. Experimental and numerical study to determine the relationship between tensile strength and compressive strength of concrete. *Civ. Eng. J.* **2018**, *4*, 2787–2800. [CrossRef]